

**The nebular spectra  
of the hypernova SN 1998bw  
and evidence for asymmetry**

Paolo A. Mazzali<sup>1,2</sup>, Ken'ichi Nomoto<sup>3,2</sup>,  
Ferdinando Patat<sup>4</sup>, and Keiichi Maeda<sup>3</sup>

Received \_\_\_\_\_; accepted \_\_\_\_\_

---

<sup>1</sup>Osservatorio Astronomico di Trieste, via G. B. Tiepolo 11, I-34131 Trieste, Italy;  
mazzali@ts.astro.it

<sup>2</sup>Research Center for the Early Universe, School of Science, University of Tokyo, Tokyo  
113-0033, Japan

<sup>3</sup>Department of Astronomy, School of Science, University of Tokyo, Tokyo 113-0033,  
Japan; nomoto@astron.s.u-tokyo.ac.jp

<sup>4</sup>European Southern Observatory, Karl-Schwarzschildstr. 2, D-85748 Garching, Germany;  
fpatat@eso.org

## ABSTRACT

The nebular spectra of the energetic Type Ic supernova SN 1998bw (hypernova) are studied. The transition to the nebular phase occurred at an epoch of about 100 days after outburst, which is assumed to coincide with GRB980425. Early in the nebular epoch the spectra show the characteristics of a typical SN Ic spectrum, with strong lines of [O I], Ca II and Mg I], and lines of [Fe II]. However, the [Fe II] lines are unusually strong for a SN Ic. Also, lines of different elements have different widths, indicating different expansion velocities. In particular, iron appears to expand more rapidly than oxygen. Furthermore, the [O I] nebular lines decline more slowly than the [Fe II] ones, signalling deposition of  $\gamma$ -rays in a slowly-moving O-dominated region. These facts suggest that the explosion was aspherical. The absence of [Fe III] nebular lines can be understood if the ejecta are significantly clumped. A schematic picture of what this very unusual stellar explosion may have looked like is presented.

*Subject headings:* supernovae: individual: SN 1998bw - nucleosynthesis

## 1. Introduction

SN 1998bw was a very interesting object from the word go (e.g. Nomoto et al. 2001). Discovered in the error box of GRB980425, and very possibly linked to it, this object was soon identified to be a supernova (SN) from its light curve, which was different from those of typical optical transients of GRB’s. Extensive data were collected at ESO, where SN 1998bw was designated a Target of Opportunity (Galama et al. 1998; Patat et al. 2001), and at other observatories.

Early spectra were rather blue and featureless, quite unlike those of other known SNe. However, a somewhat more careful inspection showed clear similarities with the spectra of Type Ic SNe (SNe Ic), but with one major difference: the absorption lines were so broad in SN 1998bw that they blended together, giving rise to what could even be confused with an emission spectrum. Very large expansion velocities ( $\sim 30,000 \text{ km s}^{-1}$ ) were measured in the ejecta. Also, SN 1998bw was very bright for a SN Ic: for a redshift distance of 39 Mpc ( $z = 0.0085$  and  $H_0 = 65 \text{ km s}^{-1} \text{ Mpc}^{-1}$ ), the SN reached a maximum  $V = -19.4$  mag, which is bright even for a SN Ia, while a typical SN Ic like SN 1994I was almost 2 mag dimmer (e.g. Nomoto et al. 1994; Richmond et al. 1996).

Modelling of the early data (Iwamoto et al. 1998, hereafter IMN98) led to several striking conclusions. First, the SN produced about  $0.7M_{\odot}$  of  $^{56}\text{Ni}$ , as much as a SN Ia. This was necessary to power the light curve via the deposition of the  $\gamma$ -rays emitted in the decay of  $^{56}\text{Ni}$  into  $^{56}\text{Co}$  and  $^{56}\text{Fe}$ .

IMN98 discuss that the light curves are degenerate, i.e. different combinations of ejecta mass  $M_{\text{ej}}$  and kinetic energy  $E_{\text{kin}}$  can all reproduce the data equally well. Spectra came to the rescue then: spectrum synthesis showed that the only way to get the observed extensive line blending was to have significant amounts of material moving at very large velocities. Since models with different  $E_{\text{kin}}$  give different degrees of blending, it was possible to select

as best model one with  $M_{\text{ej}} = 10.9M_{\odot}$  and  $E_{\text{kin}} = 3 \cdot 10^{52}$  erg. This had an exploding core mass of  $13.8M_{\odot}$  and was designated CO138 accordingly. A typical SN Ic has  $M_{\text{ej}} = 1M_{\odot}$ , and the typical kinetic energy of most SNe of all types is only about  $10^{51}$  erg (aka 1 foe). An even higher value of 50 foe was obtained for SN 1998bw by Nakamura et al. (2001a). This gives a better fit to the declining part of the light curve and to the spectra. A comparable value was obtained by Branch (2001) from an analysis of the early time spectra. Because of its exceptionally large  $E_{\text{kin}}$ , SN 1998bw was called a ‘hypernova’. The progenitor must have been a massive star, and we estimated a main sequence mass of about  $40M_{\odot}$ . Also, the remnant mass, which is computed by allowing only as much of the  $^{56}\text{Ni}$  produced by core Si burning to be ejected as is necessary to power the SN light curve, turned out to be  $\sim 3M_{\odot}$  Nakamura et al. (2001a,b). This exceeds the maximum mass of a Neutron Star, suggesting that the explosion that was observed as SN 1998bw resulted in the creation of a Black Hole.

Since SN 1998bw was probably connected to a highly non-spherical event like a GRB, departure from spherical symmetry could be expected. Early polarization measurements confirmed this. Polarization of  $\sim 0.5\%$ , possibly decreasing with time, was detected (Kay et al. 1998, IMN98, Patat et al. 2001). This was interpreted as an axis ratio of about 2:1 in the expanding ejecta (Höflich et al. 1999). Models of the collapse of a rotating stripped core of a massive star were developed, which confirmed that the explosion should be asymmetric, thus establishing a possible link with the GRB (MacFadyen & Woosley 1999).

All the above conclusions were based on only about two months worth of data. Patat et al. (2001) presented extensive data covering more than one year. Note that here and throughout the paper epochs refer to the SN time since outburst, which is taken to have coincided with GRB980425, corrected for time dilation (the host galaxy of SN 1998bw, ESO 184-G82, has a redshift  $cz = 2532 \text{ km s}^{-1}$ ), while Patat et al. (2001) used the time from  $B$  maximum, which occurred on 10 May, 1998). The evolution of SN 1998bw after

the first two months reserved several surprises: after day 60 the light curve began declining less steeply than the model prediction (Mc Kenzie & Schaefer 1999); the nebular spectrum, which started to develop after about day 100, initially appeared to be a composite of a SN Ia and a SN Ib/c spectrum, showing strong Fe lines in the blue, typical of SNe Ia, and strong O and Ca lines in the red, typical of SNe Ib/c. What was even more peculiar was that there were two families of lines: one with a large velocity comprising mostly the Fe II lines, and another with a smaller velocity ([O I], Mg I]). Also, the various lines declined with different rates, which apparently contradicts the hypothesis that the only heating source is the decay of  $^{56}\text{Co}$  (Patat et al. 2001).

Several papers have addressed the behaviour of the light curve over the first 200 days (Mc Kenzie & Schaefer 1999), 600 days (Sollerman et al. 2000) and up to 800 days (Nakamura et al. 2001a). In all these papers the suggestion has been made that either the density distribution computed in spherically symmetric explosion models is not correct or that some degree of asymmetry in the explosion is probably required to explain the unusual behaviour of the light curve. In this paper we focus on the late time spectra, and show that they too require significant asymmetry in the ejecta.

## 2. Nebular spectra

As discussed by Patat et al. (2001), the transition from photospheric to nebular spectra took place between about day 65 and day 115, although net emission may have been present in the Ca II IR triplet as early as day 37. Later other Ca II lines, the H&K doublet and the forbidden 7320Å line became visible, followed by lines of [O I], Mg I], by Na I D and by an emission at  $\sim 5200\text{Å}$ . This is most likely due to a complex of [Fe II] lines, although at the earliest phases a possible contribution is present from permitted Fe II transitions, which can produce nebular emission at sufficiently high density (Filippenko 1989), and most likely

also from [O I] 5577Å. At about day 115 the spectrum of SN 1998bw was an interesting hybrid between that of a SN Ia (strong [Fe II]) and that of a SN Ib/c (very strong [O I], Mg I], Ca II). This is already an indication that both Fe and the  $\alpha$ -elements are present with significant abundances in the ejecta. Another SN Ic for which an intense blue flux has been observed in the nebular epoch is SN 1999dq (Matheson et al. 2000a). This blue flux has been attributed to Fe II lines, but the wavelength coincidence of this feature with the [Fe II] one in SN 1998bw makes the [Fe II] identification also a serious possibility. SN 1999cq was a bright SN Ic (at least using a redshift distance), so the presence of a larger amount of Fe than in ‘normal’ SNe Ic is to be expected.

The nebular spectra span epochs from 108 to 388 days. In all the spectra six dominant features can be identified: Mg I] at 4500Å (1), the [Fe II] complex near 5250Å (2), Na I D at 5900Å (3), [O I] 6300Å (4), a [Ca II]-[O II] blend near 7200Å (5) and the Ca II IR triplet near 8500Å (6). However, although these features persist for almost one year, the change in the properties of the spectrum are striking. In particular, the [O I] and Mg I] lines become stronger relative to the [Fe II] lines as time goes on, but at the same time they also become narrower. While in the first spectrum all lines are broad ( $v \sim 12000 \text{ km s}^{-1}$ ), already in the second spectrum [O I], Mg I] and partly also Ca II IR are narrower than the [Fe II] complex. This behaviour continues for the duration of our spectral coverage, throughout which the [O I] and Mg I] lines and the [Ca II]-[O II] blend grow in strength relative to the other three features. In practice, the decline rates of the various emission lines are different, so that while in the first spectrum features (1), (2), (4) and (6) all have similar peak fluxes, and feature (5) is as strong as feature (3), in later spectra [O I] is the strongest line by far, while the [Fe II] feature rapidly decreases in strength relative to the other lines, so much so that after about one year the spectrum of SN 1998bw would be very difficult to distinguish from that of a normal SN Ib/c (see Patat et al. 2001 for a direct comparison and Matheson et al. 2001 for lots of late-time spectra of SNe Ic). At late epochs the strength

of the [O I] and Mg I] lines is mostly due to the narrow component, which develops with time but is absent in the [Fe II] feature. All the lines that decline slowly become eventually significantly narrower than the [Fe II] features. The weak Na I D line also has a narrow profile, and declines relatively slowly, while the Ca II IR triplet is almost as broad as the [Fe II] feature and declines almost as fast. The decline of the ratio Ca II IR/[Ca II] 7300Å is to be expected in a nebula of progressively decreasing density (Ferland & Persson 1989).

The features described above persist for the entire period sampled, the only noticeable change being that the [Fe II] feature moves bluewards by about 130Å between day 108 and day 214. This may be due to a decreasing contribution of an underlying ‘photospheric’ component, which is probably still significant at blue wavelengths in the earlier epochs, and to a progressively decreasing contribution of permitted Fe II emission, as the density decreases, and of [O I] 5577Å, which has a rather high excitation potential (its lower level is the upper level of [O I] 6300Å), and whose strength should decline as the electron temperature drops. After day 214, though, the emission feature stops moving, and its identification as the same [Fe II] feature observed in SNe Ia is beyond doubt (Patat et al. 2001, Fig. 11). However, the decline rate of the luminosity of the [Fe II] feature remains larger than that of both [O I] and Mg I] at all epochs (Patat et al. 2001, Fig. 14), and so this is not just due to changing contributions to the [Fe II] feature.

Another feature which receives different contributions is Na I D. Early in the nebular phase the ground state [Co III] multiplet near 5900Å contributes to this line, as it does in SNe Ia. However, the contribution is smaller in SN 1998bw because of the lower degree of ionisation. In fact, in our models Na I D is responsible for about 80% of the observed feature. At later times the contribution of Co III is further reduced because  $^{56}\text{Co}$  decays to  $^{56}\text{Fe}$ . This feature may also receive a contribution from He I 5876Å, which may be excited non-thermally since He and  $^{56}\text{Ni}$  coexist in the ejecta (Maeda et al. 2001, Fig.1).

At all epochs, the strength of the [Fe II] feature is unusually large for a SN Ib/c. Patat et al. 2001 (Fig.11) compared the nebular spectrum of SN 1998bw with that of the SN Ic 1996aq at an epoch of about 9 months, showing that in SN 1998bw the entire blue part of the spectrum, where the [Fe II] lines are important, is much stronger relative to the [O I] and Ca II lines in the red. Spectra of SNe Ic at an epoch of about 5 months, corresponding to the epoch when the spectrum of SN 1998bw had just turned nebular, have been published by A. Filippenko and collaborators (Filippenko et al. 1990 (SNe 1985F, 1987M); 1995 (SN 1994I); Matheson et al. 2001 (SNe 1990U, 1990aa)), and a comparison by eye of their spectra to those of SN 1998bw confirms the relative strength of the [Fe II] feature in SN 1998bw even at the earlier epoch.

These properties of the late-time spectrum of SN 1998bw are odd in many respects. First, all (spherically symmetric) evolution-collapse-explosion models predict that O, which is found in the unburned part of the ejecta, is located above Fe in mass coordinates. Therefore O should have a larger velocity than Fe if anything, but not a smaller one. Secondly, if the spectrum is powered by  $\gamma$ -ray deposition, the region of the ejecta which should feel the heating the most should coexist with Fe, which is mostly the product of the decay of  $^{56}\text{Co}$ . Therefore, all lines should have a similar width, that of the Fe lines, and they should decline at about the same rate. This is the case for SNe Ia. The next odd fact is that SN 1998bw had broad [Fe II] lines like SNe Ia, but lacked the strong [Fe III] peak near  $4700\text{\AA}$ , which is the strongest line in the nebular spectra of SNe Ia. If the [Fe II] identification is correct, the absence of [Fe III] clearly must be the result of a different (lower) degree of ionisation in SN 1998bw. The above facts indicate that something unusual must be going on with the way the spectrum is powered.

We used a NLTE code to compute the nebular spectrum of SN 1998bw. The code computes the deposition of the  $\gamma$ -rays from the decay of  $^{56}\text{Co}$  to  $^{56}\text{Fe}$  in a nebula of uniform



density and composition. Together with the positrons, which are also produced in the decay of  $^{56}\text{Co}$  and which are assumed to be trapped, this provides heating to the nebula. Cooling by nebular line emission is computed, a matrix of level populations is solved in NLTE and an emission spectrum is obtained. This approximation is reasonable for SN Ia nebulae (Axelrod 1980), so we apply it also to SN 1998bw. It is reasonable to do so as long as the nebular spectrum of SN 1998bw is mostly powered by  $^{56}\text{Co}$  decay. Furthermore, the density in the explosion model CO138, which reproduces the early light curve and spectra of SN 1998bw, is actually flat below about  $12,000 \text{ km s}^{-1}$  (Nakamura et al. 2001a), and mixing in the ejecta appears to be required because a stratified abundance distribution gives nebular lines with a flat-top profile (see Mihalas 1978, p.477), which is inconsistent with the observations (Sollerman et al. 2000). Mixing was also adopted in the light curve models of IMN98. Masses of the various elements are given as input to the code.

We modelled 5 spectra of SN 1998bw, dating from three months after maximum, when the SN was still entering the nebular phase, to more than one year after maximum.

Since our code assumes a uniform density, it can be used to determine the outer velocity of the nebula by fitting the width of the emission features, including complex blends like [Fe II], which is the broadest feature in all the nebular spectra of SN 1998bw. Because line blending is computed, the comparison of the widths of synthetic and observed emission features is realistic. We found that the velocity of the [Fe II] feature decreased only marginally, from  $12,000 \text{ km s}^{-1}$  in the first spectrum to  $10,000 \text{ km s}^{-1}$  in the last two, indicating that  $\gamma$ -ray deposition slowly became less efficient in the outer part of the nebula.

The major difficulties in reproducing the spectra were the presence of the narrow lines, in particular [O I] and Mg I], and the apparent absence of [Fe III] lines. As for the narrow lines, we chose to fit their peak flux, thus deriving an upper limit to the masses of these elements. The absence of [Fe III] lines is interesting. Typical models of the nebula have

electron density  $n_e \sim 10^7 \text{ cm}^{-3}$ , electron temperature  $T_e \sim 7000 \text{ K}$ , and a ratio Fe III/Fe II  $\sim 0.5$ , so that both [Fe II] and [Fe III] lines are strong. This situation is typical also in SNe Ia. The only way to decrease the strength of the [Fe III] lines without also reducing that of the [Fe II] lines is of course to decrease the ionisation. This can only be achieved by increasing  $n_e$  to favour recombination. Iron is not the main contributor to the electron density because of its relatively low abundance, so increasing  $n_e$  does not mean increasing Fe III/Fe II significantly.  $n_e$  cannot be increased by simply increasing the density, as this would imply increasing the mass, which would result in more emission in all lines.

One solution is to introduce clumping in the ejecta. This is done using the concept of volume filling factor. In practice, the state for a mass  $M$  is computed using a volume  $fV$ , where  $V$  is the entire volume of the nebula, computed from the outer velocity and the time since outburst, and  $f$  is the volume filling factor, with  $0 < f \leq 1$ . With this approximation, the density of the gas is increased by a factor  $f$  to simulate clumping. The full volume  $V$  is then used to distribute line emissivity and to compute the spectrum, which corresponds to the assumption of uniformly distributed clumps. We found that for a filling factor of about 0.1,  $n_e$  (averaged over the whole nebula) increases to  $\sim 3 \cdot 10^7 \text{ cm}^{-3}$ , while  $T_e$  drops to  $\sim 6000 \text{ K}$ , producing a lower Fe II/Fe III ratio of 0.05-0.1, which successfully eliminates the [Fe III] lines, especially at the more advanced epochs. The presence of clumping is not surprising in the ejecta of core-collapse SNe (e.g. Spyromilio et al. 1993 for SN 1987A and Spyromilio 1994, Matheson et al. 2000b for SN 1993J). Sollerman et al. (2000) using a detailed density distribution in spherical symmetry obtained a lower degree of ionisation in the Fe-rich part of the ejecta, but they had to reduce the ejecta velocity artificially with respect to the results of the explosion models in order to obtain a good agreement with the width of the observed lines. Our models for the epoch they also modelled, day 139, are similar to theirs, providing perhaps a slightly better fit in the blue region where the [Fe III] lines form. We also confirm the absence of lines of Fe I.

The properties of our models fitting the broad [Fe II] feature are summarised in Table 1, and the synthetic spectra are compared to the observed ones in Figure 1.

For all the ‘broad’ models, the  $^{56}\text{Ni}$  mass was about  $0.65M_{\odot}$ . This is in good agreement with the light curve calculations, although it is perhaps a slight overestimate since there is more flux in the synthetic spectra than there is in the observed ones, owing to the fact that the narrow observed lines are reproduced as broad lines. It is also encouraging that the  $^{56}\text{Ni}$  mass is very nearly constant over the entire period, showing that the [Fe II] feature is indeed due to  $\gamma$ -ray deposition in an expanding nebula.

The O mass, on the other hand, ranges between 3 and  $5M_{\odot}$  in the various models, increasing first and then decreasing. In the first spectrum the profile of [O I] 6300Å is broad, and so our estimate ( $M(\text{O}) \sim 3M_{\odot}$ ) is probably more realistic, considering the large errors which are always incurred in when determining the mass of O from that line (Schlegel & Kirshner 1989). However, at later times the narrow component dominates, our broad synthetic [O I] lines have a larger EW than the observed lines, and our O masses are certainly overestimated. At very late phases the O mass drops again to about  $3M_{\odot}$ , but this may be just an artifact of using a constant density model with a given velocity radius when the real ejecta had a decreasing density and so effectively a velocity radius decreasing with time.

The fact that the narrow lines of [O I] and Mg I] decline less rapidly in luminosity than the [Fe II] feature with time appears to indicate that there is a significant amount of these elements at low velocity. The ratio of the [Fe II] feature and the broad component of [O I] 6300Å in the spectrum at day 108 also suggests that the Fe/O ratio is larger at high velocity. All this is very difficult to reconcile with the classical picture of a spherically symmetric explosion, even taking into account mixing.

Sollerman et al. (2000) computed a nebular spectrum for day 139 using the original

density and abundance distributions of model CO138 (IMN98), and obtained broad [OI] lines with a flat emission top. This is a consequence of distributing O in a shell at high velocity. They overcame this problem by mixing the composition to eliminate the flat tops and by arbitrarily decreasing the velocity of the outer part of the nebula to reduce the width of the [O I] lines. However, our code can only handle nebulae of uniform density. Thus, in an alternative set of models we tried to fit the narrow-line spectrum, assuming it is also powered by  $\gamma$ -ray deposition. Such models were computed only for the last four epochs, since in the first spectrum the narrow [O I] line is still weak. The parameters of the models are detailed in Table 2, and the synthetic spectra are shown in Figure 2.

The synthetic narrow-line spectra fit well the lines of Mg I], Na I D and [O I]. The width of the lines decreases only slowly with time, as was the case for the broad [Fe II] feature: velocities range from 7500 to 5000 km s<sup>-1</sup>. The synthetic [Fe II] feature is in these models significantly too narrow. Therefore we chose to reproduce its peak only. Once again we found that the <sup>56</sup>Ni mass is very nearly constant in all four models, with a value of  $\sim 0.35M_{\odot}$ . However, this is certainly an underestimate, as the total flux in the [Fe II] feature is not reproduced. Values of the O mass in the low velocity nebula range between 1.5 and 2.7 $M_{\odot}$ , with the estimate decreasing with time after day +201. O masses which decrease with time were also derived by Schlegel & Kirshner (1989) for the SNe Ib 1984L and 1985F and for the SN II 1980K.

An upper limit to the O mass can also be derived from the flux in the [O I] 6300Å line and the nebular temperature in the high density limit ( $n_e \geq 10^6\text{cm}^{-3}$ ) using the formula

$$M(\text{O}) = 10^8 d^2 F([\text{O I}]) e^{2.28/T_4} \quad (1)$$

(Uomoto 1986), where  $M(\text{O})$  is the O mass in  $M_{\odot}$ ,  $d$  is the distance to the SN in Mpc,  $F$  is the flux of the [O I] line in erg cm<sup>-2</sup> s<sup>-1</sup> and  $T_4$  is the temperature of the nebula in units of 10<sup>4</sup>K. The high density limit should apply given the conditions in our model nebulae

(Tables 1 and 2).

The values we obtained for SN 1998bw ( $d = 39.3\text{Mpc}$ ) using values of  $T_4$  as derived from our models are listed in Table 3. The O mass thus derived is in good agreement with that used in the model calculations, except at the latest epochs, when the density is lower and the condition of Eq.(1) is not as well satisfied.

### 3. A ‘portrait’ of SN 1998bw

Most of the work on SN 1998bw has been based on spherically symmetric models. The very bright and relatively broad light curve of SN 1998bw can be reproduced by a family of explosion models with various values of the fundamental parameters ( $M_{\text{ej}}$ ,  $E_{\text{kin}}$ ). All models require  $M(^{56}\text{Ni}) \sim 0.4 - 0.7M_{\odot}$  to power the bright light curve peak. This is about one order of magnitude larger than in typical core-collapse SNe. Models with different  $E_{\text{kin}}$  yield different synthetic spectra, and by comparing with the observed early-time spectra of SN 1998bw and trying to fit the very broad absorption features, Nakamura et al. (2001a) selected a model with  $M_{\text{ej}} = 10.9M_{\odot}$ ,  $E_{\text{kin}} = 5 \cdot 10^{52}$  erg (model CO138E50). This model has the same  $M_{\text{ej}}$  but a larger  $E_{\text{kin}}$  than the model CO138 of IMN98, and it yields a better fit to the observed bolometric light curve, the evolution of the photospheric velocity and the spectra of SN 1998bw. The large value of  $E_{\text{kin}}$  easily qualifies SN 1998bw as ‘the’ Type Ic Hypernova. The mass of the exploding CO star was  $13.8M_{\odot}$ , which implies a main sequence mass of  $\sim 40M_{\odot}$ . Similar results were also obtained by Branch (2001) from models of the early time spectra.

These explosion models work well around maximum, but the predicted light curve tail is quite a bit steeper than the observed one, starting at about 60 days and continuing until at least day 200. This signals that either these energetic models underestimate  $\gamma$ -ray

deposition at those phases or that an additional source of energy is present, or both.

The nebular spectra of SN 1998bw also had a peculiar evolution. Early on, the SN showed a ‘composite’ spectrum: [Fe II] lines, typical of SNe Ia, were strong, and so were lines of [O I] and Mg I], which are typical of SNe Ib/c. At the same time [Fe III] lines, also typical of SNe Ia, were absent. The [O I] and Mg I] lines grew stronger with time relative to the [Fe II] lines, but this was due mostly to a narrow component, which became more and more the dominant one as time progressed. The emergence of the narrow profiles occurred at about the same time as the light curve deviated from the model prediction.

The broad spectrum could be reproduced with  $M(^{56}\text{Ni}) \sim 0.65M_{\odot}$  and an outer nebula velocity of  $\sim 12,000 \text{ km s}^{-1}$ . This is consistent with the distribution of  $^{56}\text{Ni}$  in CO138E50 of Nakamura et al. (2001a), but the estimate of the  $^{56}\text{Ni}$  mass is somewhat larger here. Note, however, that the light curve obtained with CO138E50 underestimates the late time flux (Nakamura et al. 2001a, Fig.5), and so this result is not unexpected. The narrow lines have a width of only  $\sim 6,000 \text{ km s}^{-1}$ , and can be reproduced with a  $^{56}\text{Ni}$  mass of  $0.35M_{\odot}$ . The velocity of the narrow [O I] line appears to be consistent with the lower energy model CO138E10 of Nakamura et al. (2001a).

On average, our nebular models required enclosed masses of  $\sim 3M_{\odot}$  below a velocity of  $6000 \text{ km s}^{-1}$  and of  $\sim 5M_{\odot}$  below  $12000 \text{ km s}^{-1}$ . Both these values are larger than the corresponding values from model CO138 by about  $2M_{\odot}$ . This may suggest the presence of a high density inner part of the ejecta, which could explain the slow decline of the light curve between days 60 and 200, as suggested by Nakamura et al. (2001a) and Chugai (2000). A similar suggestion was made by Iwamoto et al. (1999) and Mazzali et al. (2000) for the other Type Ic hypernova, SN 1997ef. However, the two situations are different. For SN 1997ef, evidence of a high density region at low velocities came from the fact that the spectra remain photospheric for a long time, and that the photospheric velocity drops below

the velocity of the inner cutoff. In a 1-dimensional explosion model, this is the separation between the material which is ejected by the SN and the infalling matter which forms the compact remnant. In SN 1998bw the photospheric phase ends earlier, and the need for the central high density region comes from the behaviour of the light curve, and it is therefore a less direct result.

Rather strong clumping had to be introduced to increase recombination and keep the [Fe III] lines from forming. Introducing clumping may slow the light curve somewhat. The increasing strength of the low-velocity intermediate-mass element emission, however, indicates that this will not be sufficient to explain all observations. The same would apply to the approach adopted by Sollerman et al. (2000), who reduced the velocity of the ejecta, thus enhancing  $\gamma$ -ray deposition, and could thus improve the fit to both the light curve and the spectrum. Also, with this approach the [Fe II] lines are not expected ever to become broader than the [O I] line.

A more complete solution which takes into account all the observed facts should probably include the presence of asymmetry in the explosion, both geometrical and in the density distribution. If SN 1998bw was actually linked to GRB980425, the fact that the explosion was asymmetric should not be surprising. Observations indicate that a rather large mass of O-dominated material is present at low velocity. Spherical explosions do not allow that: they are very effective at ‘emptying’ the central region, and always place the unburned elements at the top of the ejecta.

A 2-dimensional explosion model was computed by Maeda et al. (2001). If the explosion is highly asymmetric, it produces large quantities of unburned material (mostly C and O) expanding at low velocity in directions away from the axis along which most of the energy was released and  $^{56}\text{Ni}$  synthesised. Our vantage point must have been very close to that axis, because we also detected the GRB, as Maeda et al. (2001) show from an analysis of

the line profiles. At early times, the fast-expanding lobes must have been much brighter than the rest, and so we observed the broad-lined spectra and the bright light curve. The fast-moving regions rapidly became thin, and soon emission lines appeared. Initially the emission lines were broad, dominated by the hyper-energetic lobes. The distribution of density and abundances in a 2-dimensional model (Maeda et al. 2001, Fig. 2) shows that in the region of the ejecta with velocities of about  $10000 \text{ km s}^{-1}$  the density contours deviate less from spherical symmetry. Therefore, early in the nebular phase, when these fast-moving regions contribute to the nebular spectrum, a sufficient amount of high velocity oxygen is present that the [O I] line can be expected to be broad. Later, though, the  $\gamma$ -rays from the fast-moving  $^{56}\text{Co}$  could escape that region more and more easily, and the inner, slowly moving, O-dominated part of the ejecta would dominate the spectrum. A smaller amount of  $^{56}\text{Co}$  is present at low velocities, but the  $\gamma$ -rays it produces are trapped more efficiently and excite the O and Mg there. At lower velocities, though, the distribution of oxygen becomes preferentially equatorial, and one expects the [O I] line to decrease significantly in width as the effective size of the emitting nebula decreases. Maeda et al. (2001) suggest that the relative width of the [Fe II] complex and the [O I] line can be explained by such a model. However, because O dominates over Fe at low velocity, the strength of the [O I] line should increase relative to that of the [Fe II] feature, as is indeed observed.

The low-velocity cutoff of the asymmetric explosion model (Maeda et al. 2001, Fig. 2) is only about  $1500 \text{ km s}^{-1}$ , which is significantly less than in the 1D models ( $5000 \text{ km s}^{-1}$  in CO138E50; Nakamura et al. 2001a, Fig.7), also because of the lower overall  $E_{\text{kin}}$  of the asymmetric models (see below). This feature of the 2D models seems to match nicely the need for a low-velocity, high-density region resulting from the behaviour of the light curve. Additional deposition in the low-velocity region of the  $\gamma$ -rays produced in the high velocity region may in turn increase the deposition function above what our spherically symmetric models could estimate, and may help explain the slowly declining tail of the light curve.



That the SN 1998bw explosion was asymmetric is not a new suggestion: first the polarization measurements indicated an axial ratio of 2-3:1 (Höflich et al. 1999), and the calculation of the explosion of a rotating core (McFadyen & Woosley 1999) also gave similar results, in an effort to explain the connection between SN 1998bw and GRB980425. More detailed results have to await detailed numerical models in two dimensions. If the explosion was asymmetric, our results for  $E_{\text{kin}}$  in spherical symmetry are overestimated, because those would only refer to the fast-moving part of the ejecta. In fact, Maeda et al. (2001) propose a model with  $E_{\text{kin}} = 10$  foe. However, the estimate of the  $^{56}\text{Ni}$  mass in the nebular epoch ( $\sim 0.5M_{\odot}$ ) is probably correct, as it should not be significantly influenced by the asymmetry as long as the ejecta are completely optically thin. In this case, in fact, every optical photon created by the deposition of  $\gamma$ -rays and positrons escapes the nebula immediately and can be observed as SN light. As for the value of  $M_{\text{ej}}$ , this can only be determined by computing light curves and spectra using 3D hydrodynamical models of the explosion (e.g. Khokhlov et al. 1999), but a careful analysis of the spectra, especially at late times, when both the fast and the slow components are observable, can yield at least approximate results.

**Acknowledgements.** This work has been supported in part by the Grant-in-Aid for Scientific Research (12640233) and COE research (07CE2002) of the Japanese Ministry of Education, Science, Culture, and Sports in Japan. It is a pleasure to thank Alex Filippenko for enlightening discussions on the late-time spectra of SNe Ic.

## REFERENCES

- Axelrod, T., 1980, Ph.D. Thesis, Univ. of California, Santa Cruz
- Branch, D., 2001, in *Supernovae and Gamma Ray Bursts*, ed. M. Livio et al. (Cambridge: Cambridge University Press), in press
- Chugai, N.N., 2000, *Astron. Letters* 26, 797
- Ferland, G.J., & Persson, S.E., 1989, *ApJ* 347, 656
- Filippenko, A.V., 1989, *AJ* 97, 726
- Filippenko, A.V., Porter, A.C., & Sargent, W.L.W., 1990, *AJ* 100, 1575
- Filippenko, A.V., et al., 1995, *ApJ* 450, L11
- Galama, T. J., et al., 1998, *Nature* 395, 670
- Höflich, P., Wheeler, J.C., & Wang, L.-F., 1999, *ApJ* 521, 179
- Iwamoto, K., et al., 1998, *Nature* 395, 672
- Iwamoto, K., et al., 1999, *ApJ* 534, 660
- Kay, L.E., Halpern, J.P., Leighly, K.M., Heathcote, S., Magalhaes, A.M., & Filippenko, A.V., 1998, *IAU Circ.* 6969
- Khokhlov, A.M., Höflich, P., Oran, E.S., Wheeler, J.C., Wang, L.-F., Chtchelkanova, & A.Yu., 1999, *ApJ* 524, L107
- MacFadyen, A.I. & Woosley, S.E. 1999, *ApJ* 524, 262
- McKenzie, E.H., & Schaefer, B.E. 1999, *PASP* 111, 964

- Matheson, T., Filippenko, A.V., Chornock, R., Leonard, D.C., & Li, W., 2000a, AJ 119, 2303
- Matheson, T., Filippenko, A.V., Ho, L.C., Barth, A.J., & Leonard, D.C., 2000b, AJ 120, 1499
- Matheson, T., Filippenko, A.V., Leonard, D.C., & Shields, J.C., 2001, AJ 121, 1648
- Maeda, K., Nakamura, T., Nomoto, K., Mazzali, P. A., & Hachisu, I., 2001, ApJ, submitted (astro-ph/0011003)
- Mazzali, P. A., Iwamoto, K., & Nomoto, K., 2000, ApJ 545, 407
- Mihalas, D., 1979, Stellar Atmospheres, 2nd ed., Freeman & Co., San Francisco
- Nakamura, T., Mazzali, P.A., Nomoto, K., & Iwamoto, K., 2001a, ApJ 550, 991
- Nakamura, T., Umeda, H., Iwamoto, K., Nomoto, K., Hashimoto, M., Hix, R.W., Thielemann, F.-K., 2001b, ApJ 555, in press
- Nomoto, K., Yamaoka, H., Pols, O.R., van den Heuvel, E.P.J., Iwamoto, K., Kumagai, S., & Shigeyama, T., 1994, Nature 371, 227
- Nomoto, K., et al. , 2001, in Supernovae and Gamma Ray Bursts, ed. M. Livio et al. (Cambridge: Cambridge University Press), in press (astro-ph/0003077)
- Patat, F. et al., 2001, ApJ 555, in press, (astro-ph/0103111)
- Richmond, M.W., et al. , 1996, AJ 111, 327
- Schlegel, E.M., & Kirshner, R.P., 1989, AJ 98, 577
- Sollerman, J., Kozma, C., Fransson, K., Leibundgut, B., Lundqvist, P., Ryde, F., & Woudt, P., 2000, ApJ 537, L127

Spyromilio, J., Stathakis, R.A., & Meurer, G.R., 1993, MNRAS 263, 530

Spyromilio, J., 1994, MNRAS 266, 61

Uomoto, A., 1986, ApJ 310, L35

Table 1. Parameters of the ‘broad’ synthetic spectra.

| date       | time from max<br>days | SN epoch<br>days | v<br>km s <sup>-1</sup> | M( <sup>56</sup> Ni)<br>M <sub>⊙</sub> | M(O)<br>M <sub>⊙</sub> | M(tot)<br>M <sub>⊙</sub> | D <sub>γ</sub> <sup>†</sup> | T <sub>e</sub><br>K | log n <sub>e</sub><br>g cm <sup>-3</sup> |
|------------|-----------------------|------------------|-------------------------|--|------------------------|--------------------------|-----------------------------|---------------------|--|
| 12 Aug 98  | +94                   | 108              | 12500                   | 0.68                                   | 3.0                    | 5.0                      | 0.31                        | 6286                | 7.76                                     |
| 12 Sept 98 | +125                  | 139              | 12000                   | 0.62                                   | 3.4                    | 5.2                      | 0.24                        | 5910                | 7.47                                     |
| 26 Nov 98  | +201                  | 214              | 11000                   | 0.68                                   | 5.0                    | 7.3                      | 0.19                        | 5092                | 7.06                                     |
| 12 Apr 99  | +337                  | 349              | 10000                   | 0.65                                   | 3.9                    | 5.4                      | 0.09                        | 4090                | 6.40                                     |
| 21 May 99  | +376                  | 388              | 10000                   | 0.65                                   | 3.2                    | 4.4                      | 0.07                        | 3874                | 6.22                                     |

<sup>†</sup> D<sub>γ</sub> is the γ-ray deposition fraction

Table 2. Parameters of the ‘narrow’ synthetic spectra.

| date       | time from max<br>days | SN epoch<br>days | v<br>km s <sup>-1</sup> | M( <sup>56</sup> Ni)<br>M <sub>⊙</sub> | M(O)<br>M <sub>⊙</sub> | M(tot)<br>M <sub>⊙</sub> | D <sub>γ</sub> <sup>†</sup> | T <sub>e</sub><br>K | log n <sub>e</sub><br>g cm <sup>-3</sup> |
|------------|-----------------------|------------------|-------------------------|--|------------------------|--------------------------|-----------------------------|---------------------|--|
| 12 Sept 98 | +125                  | 139              | 7500                    | 0.36                                   | 2.1                    | 3.0                      | 0.32                        | 5971                | 7.76                                     |
| 26 Nov 98  | +201                  | 214              | 6000                    | 0.33                                   | 2.7                    | 3.8                      | 0.28                        | 5129                | 7.43                                     |
| 12 Apr 99  | +337                  | 349              | 6000                    | 0.37                                   | 2.0                    | 3.2                      | 0.12                        | 3987                | 6.73                                     |
| 21 May 99  | +376                  | 388              | 5500                    | 0.34                                   | 1.4                    | 2.2                      | 0.09                        | 3733                | 6.61                                     |

<sup>†</sup> D<sub>γ</sub> is the γ-ray deposition fraction

Table 3. [O I] 6300Å fluxes and the O mass.

| SN epoch<br>days | model  | F([O I])<br>erg cm <sup>-2</sup> s <sup>-1</sup> | T <sub>4</sub><br>10 <sup>4</sup> K | M(O)(flux)<br>M <sub>⊙</sub> | M(O)(model)<br>M <sub>⊙</sub> |
|------------------|--------|--|-------------------------------------|------------------------------|-------------------------------|
| 108              | broad  | 6.0 10 <sup>-13</sup>                            | 0.63                                | 3.2                          | 3.0                           |
| 139              | narrow | 3.3 10 <sup>-13</sup>                            | 0.60                                | 2.1                          | 2.1                           |
| 214              | narrow | 1.4 10 <sup>-13</sup>                            | 0.51                                | 1.7                          | 2.7                           |
| 349              | narrow | 2.0 10 <sup>-14</sup>                            | 0.40                                | 0.8                          | 2.0                           |
| 388              | narrow | 6.0 10 <sup>-15</sup>                            | 0.37                                | 0.4                          | 1.4                           |

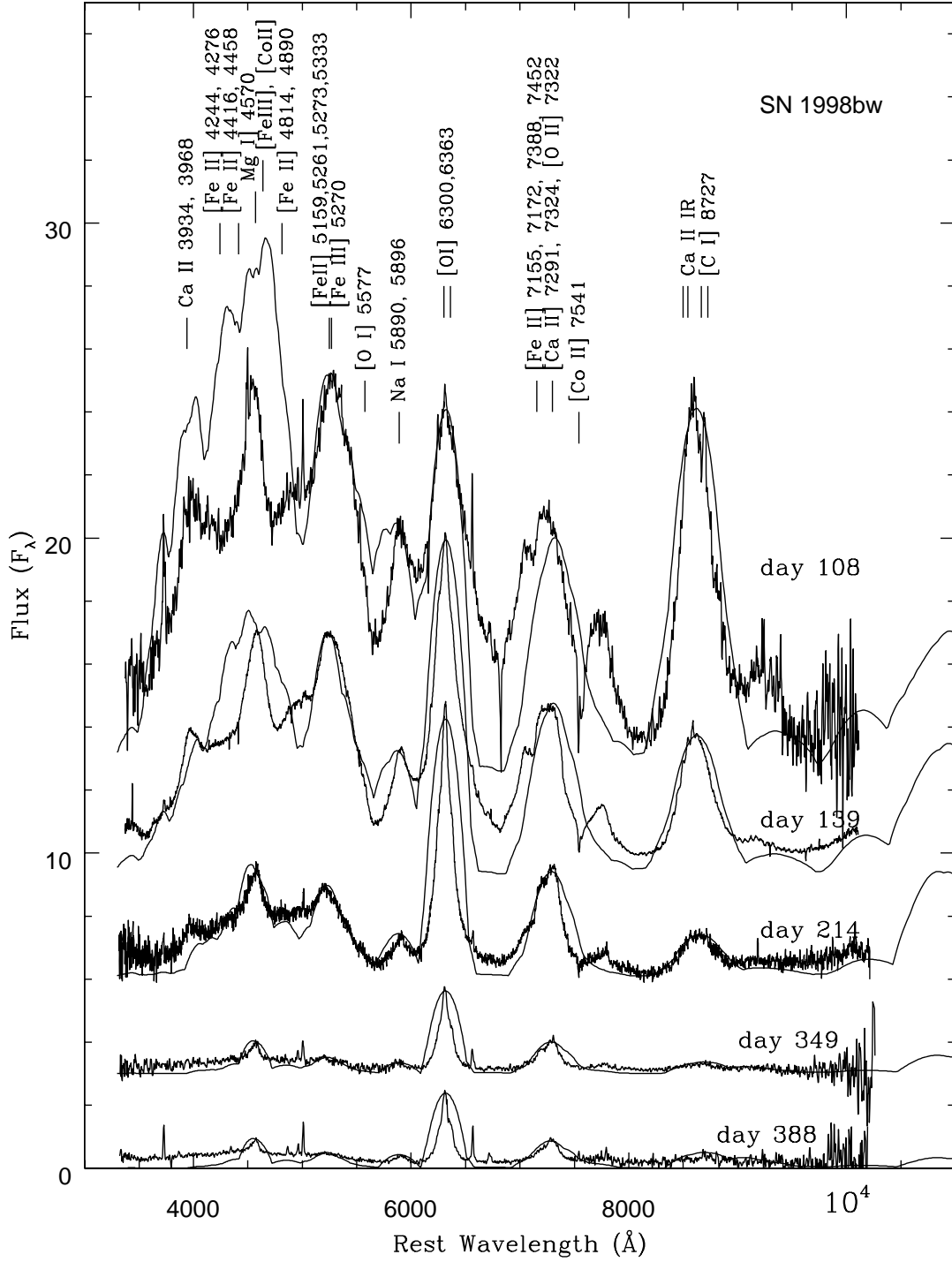


Fig. 1.— The observed spectra of SN 1998bw from 12 August 1998 to 21 May 1999 compared to the ‘broad lined’ synthetic spectra (Table 1). All spectra have been shifted arbitrarily.

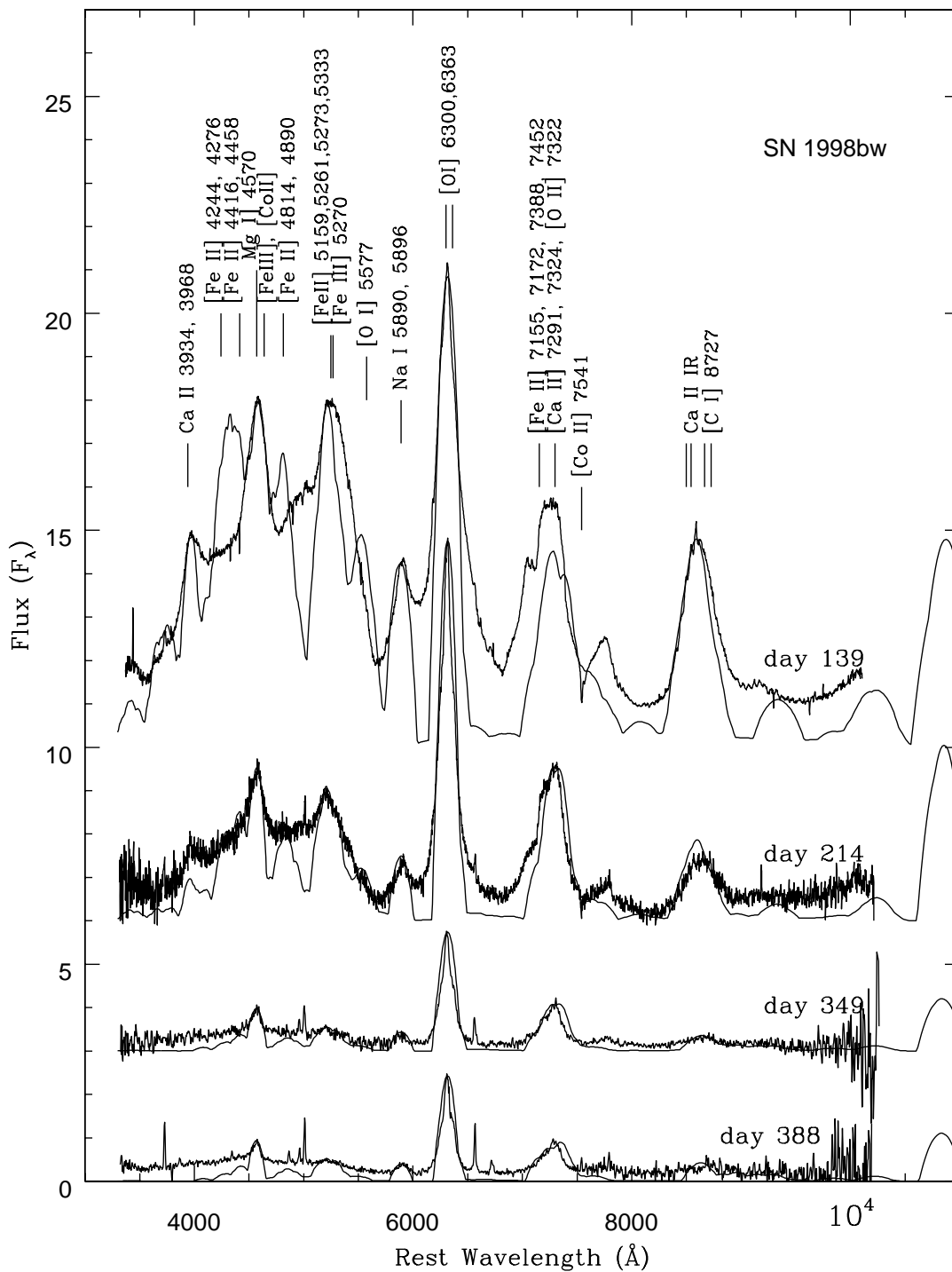


Fig. 2.— The observed spectra of SN 1998bw from 12 September 1998 to 21 May 1999 compared to the ‘narrow lined’ synthetic spectra (Table 2). All spectra have been shifted arbitrarily.